

Water Resources Research

RESEARCH ARTICLE

10.1029/2020WR027233

Key Points:

- The water year definition can change the direction of trends in streamflow timing
- By using a local water year, flood timing can often be approximated by a normal distribution
- Shifts in flood timing are systematically greater than those in the center timing of streamflow

Supporting Information:

- Supporting Information S1

Correspondence to:

C. Wasko,
conrad.wasko@unimelb.edu.au

Citation:

Wasko, C., Nathan, R., & Peel, M. C. (2020). Trends in global flood and streamflow timing based on local water year. *Water Resources Research*, 56, e2020WR027233. <https://doi.org/10.1029/2020WR027233>

Received 30 JAN 2020

Accepted 23 JUN 2020

Accepted article online 29 JUN 2020

Trends in Global Flood and Streamflow Timing Based on Local Water Year

Conrad Wasko¹ , Rory Nathan¹ , and Murray C. Peel¹ 

¹Department of Infrastructure Engineering, University of Melbourne, Melbourne, Victoria, Australia

Abstract Analysis of flood and streamflow timing has recently gained prominence as a tool for attribution of climatic changes to flooding. Such studies generally apply circular statistics to the day of maximum flow in a calendar year and use nonparametric linear trend tests to investigate changes in flooding on a local or regional scale. Here we investigate both the center timing of streamflow and the day of maximum flow using a local water year. For each station, the start of the water year is defined as the month of lowest average monthly streamflow. This definition of water year prevents ambiguity in the direction of computed trends and enables flood and streamflow timing to be described by a normal distribution. Using the assumption of normality, we calculate the historical trend in both flood and streamflow timing using linear regression. While shifts in flood and streamflow timing are consistent with climate change and are shifting in a similar direction, shifts in the timing of the annual maxima flood are approximately three times that of streamflow timing. The results here have implications for water resources and environmental management where streamflow and flood timing are critical to planning. The applicability of the normal approximation to flood and streamflow timing will enable future analyses to use parametric statistics.

1. Introduction

Analysis of flood timing informs the understanding of flood generation mechanisms related to peak rainfalls (Black & Werritty, 1997; Koutroulis et al., 2010; Parajka et al., 2010), antecedent soil moisture conditions (Berghuijs et al., 2016, 2019; Ganguli et al., 2019), and snowmelt (Burn, 1994; Matti et al., 2017; Vormoor et al., 2015). Flood timing is also used to identify climatically homogenous regions (Burn, 1997; Formetta et al., 2018; Hall & Blöschl, 2018; Ouarda et al., 2006) and detect shifts due to climate change (Burn, 1994; Matti et al., 2017; Zhang et al., 2017). Small shifts in the seasonality of floods and streamflow can have significant environmental consequences (Diehl, 2018) including changing the risk of flooding, reducing farming productivity (Klaus et al., 2016), and impacting water supply reliability (Barnett et al., 2005).

Due to the small signal-to-noise ratio, identifying trends in flood magnitude in anthropogenically unaffected catchments in response to climate change has proved challenging (Hall et al., 2014). Hence, as an alternative, it has long been argued that if climatic change is to impact flooding, then shifts in flood timing should be detectable (Schwarz, 1977). As temperatures increase under increased greenhouse gas concentrations, it can be expected that snowmelt will occur earlier (Trenberth, 2011) shifting the flood date to earlier in the year (Blöschl et al., 2017; Parajka et al., 2010). Similarly, as antecedent soil moisture is closely linked to flood occurrence (Berghuijs et al., 2019; Trambly et al., 2010; Wasko & Nathan, 2019), any sustained shift in rainfall with climatic change will change the amount of moisture in the soil and hence shift flood timing (Black & Werritty, 1997).

Changes in streamflow and flood timing are generally investigated using circular statistics. The application of circular statistics for streamflow dates back to when Gumbel (1954) applied a symmetric von Mises distribution (von Mises, 1918) to Derwent River England mean monthly streamflow. Flood timing can be approximated by a circular symmetric distribution for a majority of stations across the continental United States (Villarini, 2016). After calculating the date of flood occurrence, if the distribution of flood occurrence is non-uniform, a trend analysis can be performed. Trends can be calculated using circular-linear associations (Villarini, 2016), circular regression (Wasko et al., 2020), or the data can be adjusted and trends assessed using linear nonparametric techniques such as the Mann-Kendall trend test (e.g., Burn, 1994; Zhang et al., 2017) or Theil-Sen slope estimator (e.g., Blöschl et al., 2017; Hodgkins & Dudley, 2006).

As flood definitions differ, here we use the term “flood” to denote the annual maximum peak daily flow. Statistically significant shifts in flood timing have been found in southeastern China; however, no consistent spatial patterns were observed (Zhang et al., 2017). In Scandinavia, a shift to earlier flood peaks is consistent with a shift from snowmelt- to rainfall-dominated flooding (Matti et al., 2017) matching predictions from climate models for Nordic areas (Vormoor et al., 2015) and Switzerland (Köplin et al., 2014), and observations in snow-dominated catchments in Canada (Burn, 1994). Flood shifts to earlier in the year in western Europe and along the Atlantic coast due to earlier soil moisture maxima have been identified, but in other regions, such as the North Sea, later winter storms are causing shifts to later flood occurrence (Blöschl et al., 2017). In Australia, flood timing demonstrated consistent regional shifts despite no sites showing statistically significant trends. Flood timing has shifted to earlier in the year in the tropical north, and to later in the year in the temperate south, consistent with changes in antecedent moisture (Wasko et al., 2020). Detecting changes in flood timing remains challenging, with the strength (nonuniformity) of flood seasonality, rather than shifts in the day of timing, more likely to show a trend (Villarini, 2016).

Shifts in streamflow seasonality are usually studied using the “center timing,” that is, the date for which half of the year’s total streamflow has passed the streamflow gauge (Court, 1962), and this is the definition adopted here. Observed shifts in streamflow (center) timing are largely consistent with the shifts in flood timing described above. For example, across eastern North America, strong evidence of shifts to earlier streamflow timing for the past century was found using the linear nonparametric Sen slope (Hodgkins & Dudley, 2006). This shift to earlier streamflow has been observed for the majority of snowmelt-dominated catchments in the United States (Dudley et al., 2017; Stewart et al., 2005) and, through attribution studies using linear regression, concluded to be in response to anthropogenic changes (Barnett et al., 2008; Hidalgo et al., 2009). Shifts to earlier seasonal streamflow and earlier ice melts have also been observed in Canada (Burn & Elnur, 2002; Najafi et al., 2017; Zhang et al., 2001). Other statistics, such as the 75th percentile of mass passing the streamflow gauge, have also identified shifts to greater and earlier streamflow in Spain (Morán-Tejeda et al., 2014). Increases in winter streamflow volumes and earlier snowmelt floods are consistent with increased temperatures in Nordic areas (Wilson et al., 2010) as well as the majority of Europe (Stahl et al., 2012).

Investigations of flood and streamflow timing will likely continue to be at the forefront of understanding flood causing mechanisms (Berghuijs et al., 2016) and identifying changes in the hydrologic cycle due to climate change (Blöschl et al., 2017; Wasko et al., 2020). Here we perform the first study to concurrently investigate the mean seasonality, (statistical) distribution, and trends in flood and center timing at a global scale. We identify that arbitrary adjustment of flood and center timing can result in ambiguous trend direction and propose the use of a consistent definition of the water year based on catchment-scale streamflow seasonality to remove this ambiguity. We identify distributional properties of flood and streamflow timing, which may be exploited in future studies. Finally, we investigate the trend in flood and streamflow timing globally to aid our understanding of the impact of climate change.

2. Data and Methods

2.1. Data and Water Year Definition

Daily streamflow from the Global Runoff Data Centre (GRDC, 2015) as successfully used in other global studies (Do et al., 2017; Lee et al., 2015; Milly et al., 2018; Wasko & Sharma, 2017; Wasko et al., 2019) was adopted here. We restrict our analysis to sites with more than 20 years or more of data resulting in a total of 4,472 sites across the world. The water year is defined locally at each gauge as the 12-month period beginning in the month of lowest average monthly streamflow. For the example of South Johnstone River (Figure 1a), the water year starts in the tenth month of the year (October). The South Johnstone River is chosen as an example because the period of rising average monthly streamflow straddles the end/start of the calendar year and will be used to demonstrate the need for appropriate adjustment below.

The ordinal day (j_i) of flood and streamflow timing is estimated using the calendar year. Flood timing is the ordinal day of annual maximum flow, and the streamflow (center) timing is defined as the ordinal day at which half of the annual flow has passed the streamflow gauge (Court, 1962). Although alternative definitions of streamflow timing exist (e.g., Lee et al., 2015), using the above center timing definition is attractive, as it provides an ordinal day, which is easily compared to the flood timing.

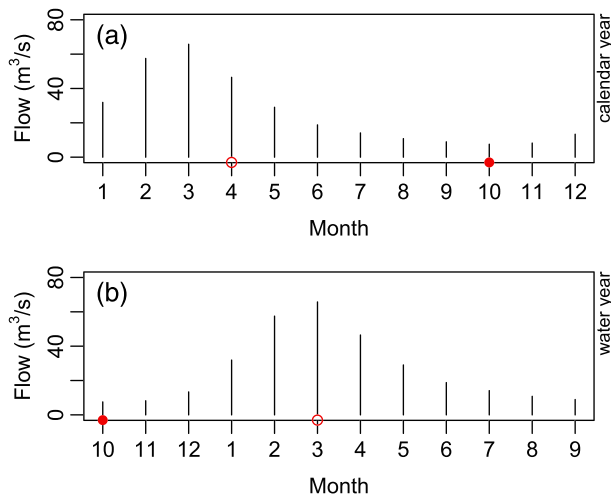


Figure 1. Histogram of mean monthly streamflow for the South Johnstone River (145.978°, -17.61°) in Australia, (a) using the calendar year and (b) using the water year. Red filled circle corresponds to the month of lowest mean monthly streamflow and hence the start of the water year. Open red circles are streamflow (center) timing estimates.

The center and flood timing are calculated for each year with zero flow years omitted. Both the flood timing and center timing can be calculated (sampled) based on the local water year. Figure 1 presents the importance of considering an appropriate local water year when sampling center timing. Suppose sampling is based on calendar year, then the center timing occurs in April (Figure 1a). This is misleading, as when calculated with the water year starting in October, the center timing occurs in the center of the streamflow seasonality, which is in March (Figure 1b). To further compound this ambiguity, suppose an increase in December streamflow, where no change in streamflow is observed in other months (Figure 1a). For the case when streamflow seasonality is considered using the calendar year, this would be interpreted as a shift to *later* streamflow center timing (Figure 1a) whereas in fact the correct interpretation, using a local water year, is a shift to *earlier* streamflow center timing (Figure 1b). This change in the interpretation of the trend direction occurs due to the choice of when the water year starts and will occur regardless of whether circular or linear statistics are used. We note this artifact is less likely to be introduced in sampling flood timing as sampling block maxima is largely invariant to block start date (as long as it is not selected to coincide with a season when floods typically occur), but as streamflow is largely nonuniform, the choice of start date for flood sampling remains important.

2.2. Circular Statistics

Circular statistics are often applied to the investigation of flood and streamflow timing as streamflow exists on a cyclical continuum. The ordinal day of an event at the end of a year is close to an event occurring at the start of the following year, but on a linear scale, these day numbers are far apart (Bayliss & Jones, 1993). To apply circular statistics, the ordinal day (j_i) needs to be converted to an angular value θ_i , where m is the number of days in the year and $i = 1 \dots n$ is the number of years.

$$\theta_i = \frac{j_i}{m} \times 2\pi. \quad (1)$$

The mean direction $\bar{\theta}$, or mean timing, in radians is then calculated by (Fisher, 1993)

$$C = \sum_{i=1}^n \cos\theta_i \quad S = \sum_{i=1}^n \sin\theta_i$$

$$\bar{\theta} = \begin{cases} \tan^{-1}\left(\frac{S}{C}\right) & S \geq 0, C > 0 \\ \tan^{-1}\left(\frac{S}{C}\right) + \pi & C \leq 0 \\ \tan^{-1}\left(\frac{S}{C}\right) + 2\pi & S < 0, C > 0 \end{cases}. \quad (2)$$

Figure 2a presents an example of this calculation. Here we continue with the example of the South Johnstone River as, based on calendar year, the flood timing distribution crosses the end-start year continuum (i.e., some floods occur in December, and the rest occur in January–May). The mean calculated using linear statistics (open circle) is biased toward the end of the year (Day 68) compared to the true mean (red circle) of Day 57, which is calculated using circular statistics (Equation 2). As the applicability of most trend tests requires a nonuniform distribution (Blöschl et al., 2017; Dhakal et al., 2015), the Rayleigh test is used, with the null hypothesis being the distribution is uniform (Fisher, 1993).

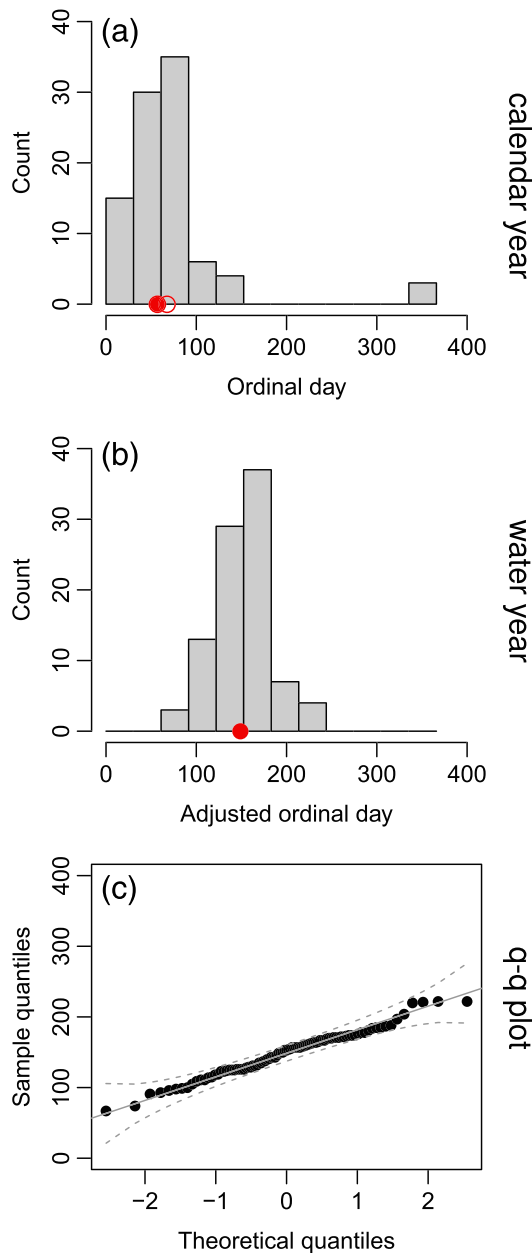


Figure 2. Flood timing for the South Johnstone River (145.978°, -17.61°) in Australia showing (a) histogram of flood timing using the calendar year, (b) histogram of flood timing using the water year, and (c) qq-plot of flood timing for normal distribution based on water year. Red-filled circles are the circular mean, while open circles are the arithmetic mean. In panel (b) the circles overlay.

2.3. Linear Statistics Based on Water Year

If a circular variable does not extend around the circle, it can be linearized without great error and can be analyzed based on normality (Court, 1952). To ensure a sequence of dependent flood events (annual maxima) is not counted in two successive years (e.g., Gumbel, 1941), the flood and center timing can hence be adjusted based on the start of the water year, which is October in the case of the example presented (Figure 2b). The number of days since the first day of the first month of the water year is then the adjusted (or standardized) ordinal day j_i^* :

$$j_i^* = \begin{cases} (j_i - z) \bmod m & j_i - z \neq m \\ m & j_i - z = m \end{cases}, \quad (3)$$

where z is the number of days from the first day of the calendar year to the first day of the water year and m is the number of days in the year. The mean flood seasonality is calculated as the arithmetic mean:

$$\bar{j}^* = \frac{1}{n} \sum_{i=1}^n j_i^*. \quad (4)$$

The arithmetic mean (Figure 2b) now aligns with that calculated using circular statistics (Figure 2a). Moreover, a shift in the center timing, for example, due to an increase in December streamflow at the beginning of the distribution, is now correctly interpreted as a shift to earlier (and not later) timing. The ordinal day of flood seasonality in units of calendar year (\bar{j}) can be obtained by the reverse of Equation 3. Normality is confirmed using the D'Agostino test of skewness (D'Agostino, 1970; D'Agostino et al., 1990). For the South Johnstone River example, the p value of 0.89 confirms that the assumption of normality cannot be rejected (Figure 2c).

2.4. Global Analysis of Flood and Center Timing

Although linear statistics are not appropriate in most cases when analysis is performed on the basis of calendar year (as shown by the example in Figure 2), they may be appropriate after adjusting to the local water year. As circular statistics have traditionally been used to investigate flow timing, a parallel analysis using circular statistics is presented in the supporting information and referred to (in the main body of the paper) for comparison with the linear approach based on adoption of a local water year, which is the focus here.

Trends in streamflow (center) and flood timing are calculated using both linear regression and the Theil-Sen slope estimator using the ordinal day of timing standardized on the local water year. The assumption of no serial correlation is tested using the Durbin-Watson test (Durbin & Watson, 1950). The Rayleigh Test for a nonuniform distribution and the D'Agostino Test of skewness for a normal distribution are applied at each site. Statistical significance is reported using a global (field) level of significance of 1% (Wilks, 2006), based on the false discovery rate (Benjamini & Hochberg, 1995), to minimize any influence on the results of spatial cross correlation between the 4,472 gauges.

3. Results

3.1. Water Year, Mean Flood Timing, and Mean Streamflow Timing

In extratropical regions of the Southern Hemisphere where there is little snow, the water year generally begins toward the start of the calendar year, that is, the end of the austral summer, or the beginning of the austral autumn (Figure 3a). In tropical regions of the Southern Hemisphere, the period of lowest flow occurs much later in the year, and hence, the start of the water year corresponds approximately to the end of the austral winter; this aligns with the highly seasonal summer rainfall that tropical regions of the world experience. In the Northern Hemisphere, as the climatic conditions are more mixed, the start of the water year varies more with geographic region. For example, on the east and west coast of the United States, the start of the water year corresponds to the boreal autumn months, but inland there are many regions where it could be argued that the calendar year is a good approximation for the water year. This highlights that the assumption of a single water year over large continental regions is unlikely to be adequate.

The start of the water year in the central United States is related to whether streamflow is snow dominated. For example, in the midwest the water year begins in the boreal winter. Although a simplification, a similar pattern of water year can be observed in Europe where mountainous regions in the Alps and snow-dominated areas in the north have the lowest streamflow in the boreal winter, and elsewhere, the water year begins toward the boreal autumn. In the United Kingdom, the lowest streamflow occurs in the summer months. Although fewer gauge sites exist in equatorial regions, the water year begins in approximately April or May, while in Japan the water year appears to follow the calendar year.

Mean flood timing calculated using the arithmetic mean of the ordinal day based on local water year (Equations 3 and 4) is presented in Figure 3b. The mean flood timing resembles similar global studies of high flow season (Lee et al., 2015) and peak flow month (Dettinger & Diaz, 2000). In northern Australia, the highest flows tend to occur at the start of the calendar year, toward the end of the austral summer. In the south the mean flood timing is mixed but generally peaks in winter. In Australia, the mean flood timing corresponds to the rainfall seasonality (Linacre & Geerts, 1997), with the trend with latitude replicated across the entire Southern Hemisphere suggesting similar flood mechanisms. The mean flood timing for the United States corresponds with previously published continental studies (Berghuijs et al., 2016; Villarini, 2016). A large amount of variability is exhibited based on local climatology. Florida experiences flooding usually in the latter half of the calendar year while the east and west coasts generally exhibit flood events toward the start of the calendar year. Throughout the central United States and Canada, melting snow appears to result in flood peaks concentrated around the boreal spring. Europe has a mean flood timing that can be generalized to spring timing where there are mountains and snow, while the United Kingdom and western Europe experience winter dominant flooding driven by wet soil moisture conditions (Blöschl et al., 2017). In equatorial regions the mean flood timing occurs in September and October corresponding to the end of the monsoon season pointing to the accumulation of soil moisture contributing to peak flood occurrence.

Because floods are the largest contributor to annual streamflow volumes, the greatest flood in the year will also have a dominant influence on center timing. The geographical distribution of the mean center timing (Figure 3c) is almost identical to the mean flood timing (Figure 3b) with a (circular) correlation (Fisher, 1993) of 0.9. As we have only considered the maximum 1-day streamflow for flood timing and not a moving average (which is often used in similar studies), and flooding tends to exhibit high variability, this correspondence is very close. In the Southern Hemisphere the mean center timing of streamflow occurs in the austral summer and in the subtropics in the austral winter. In the Northern Hemisphere the mean streamflow center timing is dictated by flood mechanism with snowmelt-driven catchments experiencing mean center timing in the boreal spring and summer and otherwise toward the end of the boreal winter.

For comparison, mean flood timing (Figure S1a) and mean center timing (Figure S1b) are calculated using circular statistics (Equation 2). There is little difference in the geographical distribution of mean flood timing to when a linear approach based on local water year is used (Figure 2). The histogram of differences (Figure S1a) suggests little bias (1 day), and 75% of sites have a difference of less than 10 days (which represents a difference of less than 3% over the length of a year). Some differences remain where, after standardization, some of the timing distribution still straddles the boundary of the water year. The comparison

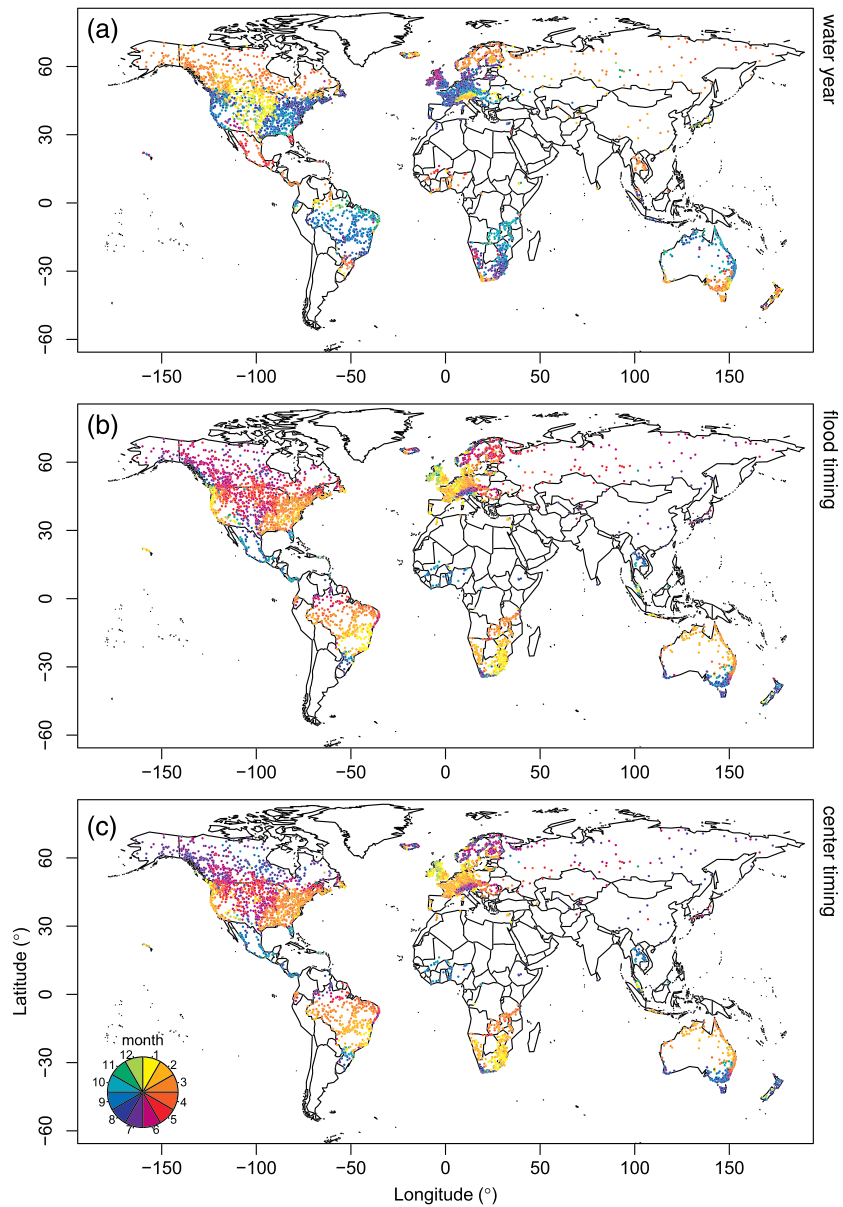


Figure 3. Streamflow timing statistics: (a) start of local water year, (b) mean flood timing, and (c) mean streamflow (center) timing. The local water year is defined as 12-month period beginning in the month of lowest mean monthly streamflow. The flood and streamflow timing are calculated using the arithmetic mean after standardizing on the water year and presented in the calendar year. The legend is the calendar year month where the first month is January.

between circular and linear approaches is almost identical for mean center timing, which could be expected, as center timing exhibits less variability than flood timing. Now 97% of sites have a difference of less than 10 days between approaches, and 82% of sites correspond by 2 days or less. This confirms that by adopting a local water year both flood and center timing can be linearized without great error (Court, 1952).

3.2. Normality and Nonuniformity of Flood and Streamflow Timing

At the 1% global (field) level of significance, the flood timing can be approximated by a normal distribution at 80% of sites, with this proportion increasing to 94% in the Southern Hemisphere (Figure 4a). This corresponds approximately to the number of sites with flood timing (92% globally and 86% in the Southern Hemisphere) that have the assumption of uniformity rejected by the Rayleigh test (Figure S2a). There is evidence that where the statistical test rejects normality in the Northern Hemisphere, the sites correspond to

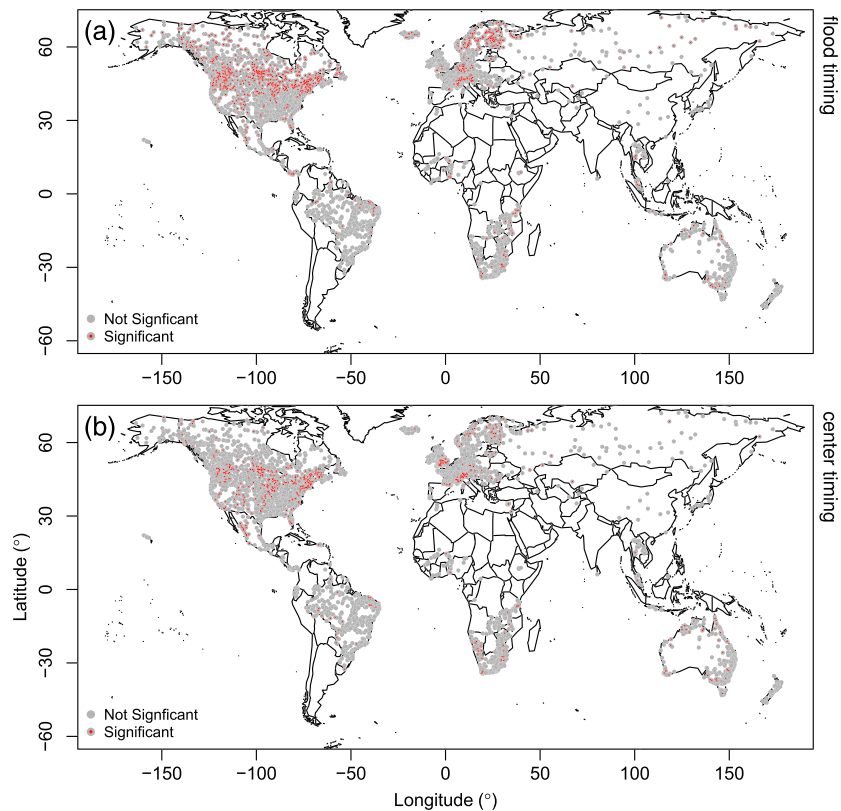


Figure 4. Test of distribution normality for (a) flood timing and (b) streamflow (center) timing. Gray dots show gauge locations. Test for normality uses the D'Agostino test with the null hypothesis that the distribution is normally distributed. Tests are performed at the 1% global (field) level of significance.

regions of snowmelt-dominated flooding, for example, North America, Nordic regions, the Swiss Alps, and Northern Italy. Due to multiple flood generation processes, flooding can occur at any time of the year in the Swiss Alps and exhibits a bimodal distribution in Northern Italy.

Flood timing is unimodal in the Nordic areas and in North America, but there is evidence of a skewed distribution of flood timing dependent on the snowmelt timing. The flood timing exhibits a strongly peaked distribution with a long tail extending to the boreal summer resulting in a positively skewed distribution. Sites in South Africa and along the southeast coast of Australia can be approximated as normal despite not being statistically different from a circular uniform distribution. This is because at these locations there is a wide spread in flood timing. The flood timing distribution is symmetric with a small peak allowing the assumption of normality despite not being statistically different from uniformity.

There are very few sites in the world where the central timing does not conform to the normal distribution. The center timing distribution can be approximated by the normal distribution at 88% of sites globally and 93% of sites in the Southern Hemisphere (Figure 4b). Globally, 99% of sites are circularly nonuniform (Figure S2b). The regions where the hypothesis test of normality fails are almost identical to that presented in Figure 4a for flood timing, which suggests that the distributions for flood timing and center timing are very similar. Representing flood and center timing using linear statistics that are approximately normal facilitates the use of a wide range of traditional statistical tests, which have greater power (require a smaller sample size) than nonparametric tests (Hipel & McLeod, 1994).

3.3. Trends in Flood and Streamflow Timing

The trend and magnitude of shifts in flood timing calculated using linear regression are presented in Figure 5. For the interested reader trends that have not been gridded are presented in Figure S3. Fewer than 1% of sites have statistically significant autocorrelation confirming sample independence. In Australia, there

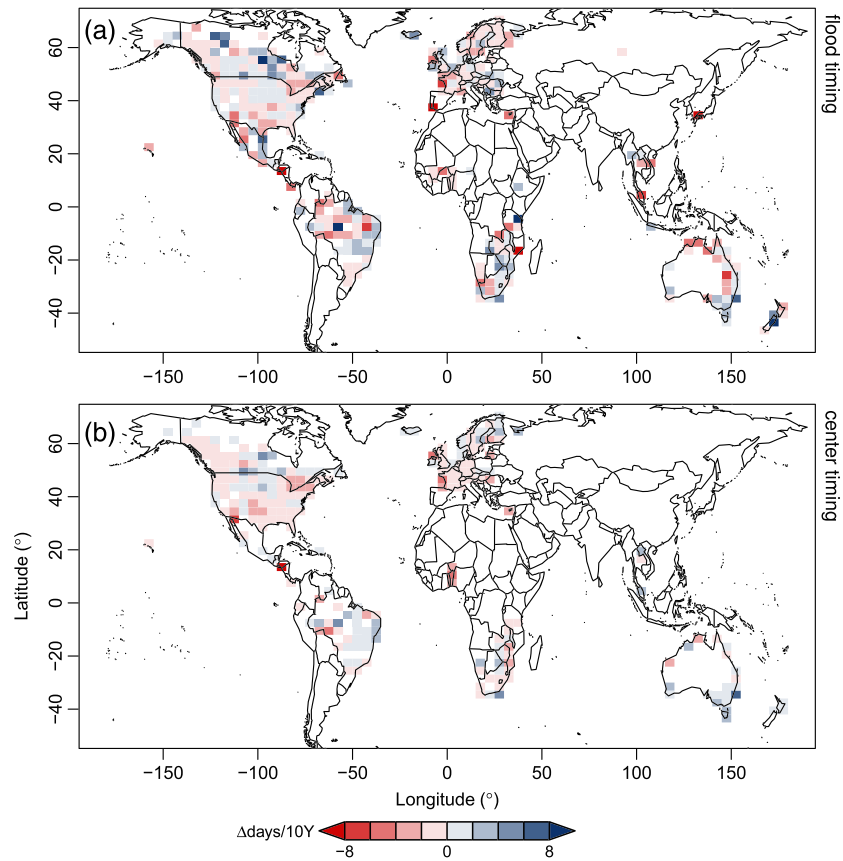


Figure 5. Trend in timing using linear regression for (a) flood and (b) streamflow (center). Each grid cell is the median trend for all the underlying stations. Only grid cells containing more than five stations were included. The trend is in ordinal days per decade, with red representing a shift to earlier in the water year and blue to later in the water year.

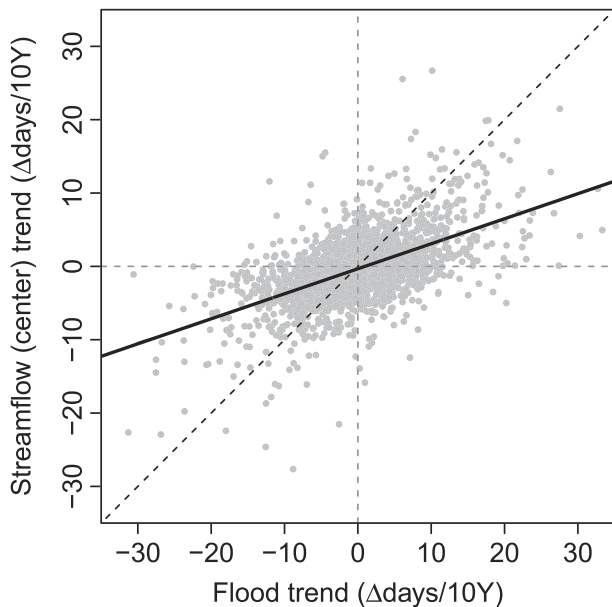


Figure 6. Scatter plot of linear regression trends in flood and streamflow (center) timing for each gauge. Only sites with more than 30 years of record are included. The thick black line is a least squares line of best fit.

is a trend to earlier flooding in the central north, possibly a result of increased mean rainfall causing the soil to saturate earlier; conversely in the south, flooding occurs later in the year, again, consistent with the decrease in mean rainfall this region is experiencing (Head et al., 2014) and it taking longer for soil to saturate delaying the onset of flooding (Wasko et al., 2020). Similar shifts to later flooding in south east Brazil are consistent with decreased mean rainfall and possible shifts in precipitation extremes to later in the year (Marelle et al., 2018; Rao et al., 2016). The converse is true in the tropical and equatorial regions where the shift to earlier flooding may be the result of increased mean rainfalls and earlier precipitation maxima.

There is evidence of earlier snowmelts causing flooding to shift earlier in the United States consistent with the expectation that warmer temperatures will increase snowmelts with climatic change (Hamlet & Lettenmaier, 2007). Although these trends are not universal, they dominate the north American continent except for the midwest, where small shifts to later flooding are identified. Throughout Europe there are shifts to earlier flooding, particularly in Nordic areas, due in part to earlier snowmelts as a result of higher temperatures (Matti et al., 2017). The United Kingdom exhibits a mixture of trends. There is evidence of later flooding in northern United

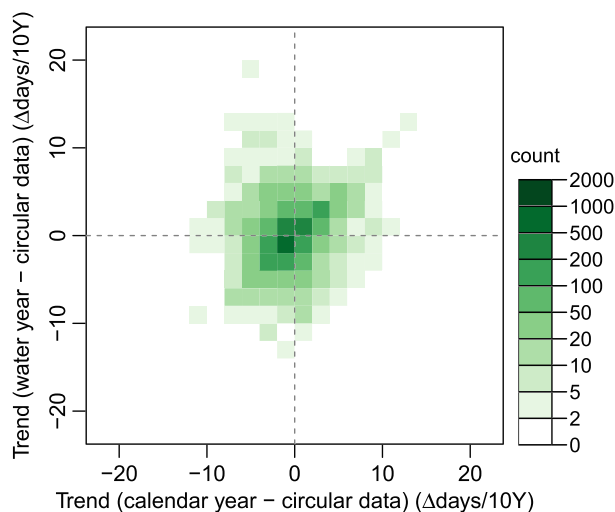


Figure 7. Trend in center timing using alternative definitions of water year. The center timing trend calculated using the calendar year and stored as circular data is on the x axis; the center timing trend calculated using the local water year is on the y axis. The trend is in ordinal days per decade. Only sites with more than 30 years of record are presented. All trends are calculated using the Theil-Sen slope estimator.

Kingdom due to later winter storms and earlier flood timing in southern United Kingdom due to earlier soil moisture maxima possibly due to later soil moisture accumulations (Blöschl et al., 2017). The trend in center timing (Figure 5b) follows the trend in flood timing (Figure 5a). Similar results were obtained using the nonparametric Theil-Sen slope estimator on data adjusted to water year (Figures S4 and S5).

Figure 6 presents a scatterplot of the magnitude of the center timing trend against the magnitude of the flow timing trend with a least squares line of best fit (r squared 0.32). The similarity in the direction of flood and center timing trends suggests that, similar to indicators of flow magnitude (Gudmundsson et al., 2019), the entire flow distribution is shifting, in this case to either earlier or later in the year. As stated previously, floods are the largest contributor to annual streamflow volumes and will have a dominant influence on center timing. The magnitude of the center timing is, on average, almost exactly one third the magnitude of the flood trend, suggesting shifts in extremes due to climate change are greater compared to mean trends. When the nonparametric Theil-Sen slope estimator is applied, instead of linear regression, the results are similar, with a slightly smaller r squared of 0.22 for the least squares line of best fit (Figure S6).

3.4. Importance of Water Year in Trend Calculation

In section 2.1 we introduced an example of where the definition of water year can change the direction of trends calculated for center and flood timing. To confirm this can happen in practice, we present a comparison of trends calculated when sampled using our definition of local water year versus the case where the calendar year is used (Figure 7). Adjustment is required to enable trend calculation after sampling on calendar year. Here, the circular mean is subtracted, and the data are adjusted to vary between $\pm\pi$. The trends are then calculated using Theil-Sen slope estimator and compared to the slope estimate when sampling is performed based on local water year. The results vary greatly with 35% of sites misclassified in terms of the trend direction. Whereas regardless of whether the trend in center timing is calculated using circular or ordinal (linear) data, the calculated trend is the same when the data are sampled on local water year (not shown). For the interested reader Figure S7 presents the center timing globally when calendar year is used. Where the streamflow generally occurs in the seasons crossing the December–January (end-start year) threshold (Figure 3c), misclassification of trend direction is apparent, for example, in the east coast of the United States and in southern Africa (cf. Figure 5b).

4. Discussion and Conclusions

We defined the local water year as the 12-month period beginning at the start of the month with lowest average monthly streamflow and presented a global analysis of streamflow (center) and flood timing based on local water year. Mean flood seasonality occurs toward the late austral summer in Southern Hemisphere tropical regions and September–October in equatorial regions corresponding to the end of the rainfall (monsoon) season. In areas of the world where streamflow is dominated by snowmelt, the mean flood timing and mean center timing occur post-snowmelt in the (boreal) spring. The mean flood and center timing correspond closely and were similar regardless of whether linear statistics after adjustment to the local water year, or circular statistics using the calendar year, were used.

Sampling center and flood timing on local water year prevents the calculation of incorrect trend direction, ensures flood events are serially independent, and results in the interesting property that center timing and flood timing are normally distributed. Here we used the assumption of independent and identically distributed random variables to perform linear regression for trend in center and flood timing. Global trends in flood timing are consistent with large-scale climatic change. Warming temperatures are leading to earlier flood peaks due to earlier snowmelts in snow-driven catchments, whereas elsewhere the flood timing may

be linked to the tropical expansion changing mean and extreme rainfalls and the time taken to saturate catchments. This has already been shown to be the case in Australia where earlier flooding is occurring in tropical regions that are getting wetter and later flooding is occurring in extratropical regions that are getting drier (Wasko et al., 2020). Similar shifts to later flooding in southeastern Brazil are consistent with drier extratropics. Across the western United States and northeastern United States, there is a dominant shift to earlier flooding likely due to earlier snowmelt associated with warmer temperatures. There is a clear trend to earlier flooding in Nordic regions, but the United Kingdom, with different flood generating mechanisms, exhibits later flooding in the north and earlier flooding in the south (Blöschl et al., 2017). Overall, trends in flood timing match trends in central timing in direction but are three times the magnitude of center timing trends, suggesting climate change is likely to exacerbate changes in extreme events relative to changes in streamflow means.

Given recent attention to the role of changing antecedent conditions affecting flooding in a nonstationary climate (Sharma et al., 2018; Wasko & Nathan, 2019) and the attribution of changes in flood seasonality to changes in the hydroclimatic drivers of flooding (Black & Werritty, 1997; Blöschl et al., 2017), we expect studies of nonstationarity in flood seasonality to continue to be of high importance. Moreover, with the continual improvement of technological resources, we expect studies using large-scale hydrologic data sets, to be at the fore of understanding climate change impacts in hydrology (e.g., Do et al., 2020; Gudmundsson et al., 2019; Stein et al., 2020). But where center timing is calculated on calendar year over large diverse geographical areas (e.g., Do et al., 2018; Gudmundsson et al., 2018), we urge caution. The large regional variation in local water year calls into question the common practice of adopting a single water year regionally or continentally (e.g., Ukkola & Prentice, 2013), especially in studies of center and flood timing. As shown here, regardless of the statistical approach adopted, adjustment of the data is still generally required for trend analysis, and an incorrect interpretation of trends is possible if this is not undertaken carefully. Hydroclimatic trend studies should use a frame of reference that is of most relevance to the natural process of interest. In the case we presented, flooding and streamflow, the frame of reference is the water year that starts with a low flow. Conversely, if the focus of interest was on droughts or low-flow periods (e.g., Young et al., 2000), then the frame of reference could be a water year that starts with a high-flow month. Trends in other climate variables such as precipitation (e.g., Gu et al., 2017; Marelle et al., 2018) or soil moisture timing (e.g., Blöschl et al., 2017; Wasko et al., 2020) should also consider an appropriate frame of reference such as that presented here.

The methods presented here do not replace nonparametric methods of investigating changes in seasonality for complex situations where the distribution of timing is multimodal (Dhakal et al., 2015). Across the northeast of the United States, annual timing in the flood rich cool season has not shifted, but increased flooding has been observed in the warm seasons, shifting flood seasonality (Collins, 2019). In Norway, greater dominance or rainfall-driven flooding will shift flood timing differently between catchments (Vormoor et al., 2015). Intraseasonal flood changes can be missed when flood timing is analyzed based on annual unimodality. In addition, due to complexity and scale-dependence of catchment response (Sharma et al., 2018; Whitfield, 2012), regional analyses such as the one presented here should not be used as a substitute for catchment scale studies where catchment flood response may differ. Rather, studies such as this one should be seen as complementary to more detailed, catchment level studies.

The methods and results presented here will continue to aid the understanding of the impacts of climate change on flood and streamflow (center) timing at a global scale. We find that adjusting the data at the beginning of the analysis on local water year can allow for a consistent approach throughout the analysis, from sampling data, through to calculating seasonality and trends. Adjusting to the local water year also has the interesting property that normality cannot be rejected for flood and center timing. This allows inferences regarding the direction of trends that are more easily interpreted than those derived using circular statistics and opens the possibility to a range of more powerful parametric statistics that could be applied in future studies.

Acknowledgments

Conrad Wasko acknowledges support from the University of Melbourne McKenzie Postdoctoral Fellowship scheme. Data are freely available from the Global Runoff Data Centre (https://www.bafg.de/GRDC/EN/Home/homepage_node.html) upon request.

References

- Barnett, T. P., Adam, J. C., & Lettenmaier, D. P. (2005). Potential impacts of a warming climate on water availability in snow-dominated regions. *Nature*, *438*(7066), 303–309. <https://doi.org/10.1038/nature04141>
- Barnett, T. P., Pierce, D. W., Hidalgo, H. G., Bonfils, C., Santer, B. D., Das, T., et al. (2008). Human-induced changes in the hydrology of the Western United States. *Science*, *319*(5866), 1080–1083. <https://doi.org/10.1126/science.1152538>

- Bayliss, A., & Jones, R. (1993). *Peaks-over-threshold flood database: Summary statistics and seasonality* (Report No. 121). Wallingford, UK.
- Benjamini, Y., & Hochberg, Y. (1995). Controlling the false discovery rate: A practical and powerful approach to multiple testing. *Journal of the Royal Statistical Society: Series B: Methodological*, 57(1), 289–300. <https://doi.org/10.2307/2346101>
- Berghuijs, W. R., Harrigan, S., Molnar, P., Slater, L. J., & Kirchner, J. W. (2019). The relative importance of different flood-generating mechanisms across Europe. *Water Resources Research*, 55, 4582–4593. <https://doi.org/10.1029/2019WR024841>
- Berghuijs, W. R., Woods, R. A., Hutton, C. J., & Sivapalan, M. (2016). Dominant flood generating mechanisms across the United States. *Geophysical Research Letters*, 43, 4382–4390. <https://doi.org/10.1002/2016GL068070>
- Black, A. R., & Werritty, A. (1997). Seasonality of flooding: A case study of North Britain. *Journal of Hydrology*, 195(1–4), 1–25. [https://doi.org/10.1016/S0022-1694\(96\)03264-7](https://doi.org/10.1016/S0022-1694(96)03264-7)
- Blöschl, G., Hall, J., Parajka, J., Perdigão, R. A. P., Merz, B., Arheimer, B., et al. (2017). Changing climate shifts timing of European floods. *Science*, 357(6351), 588–590. <https://doi.org/10.1126/science.aan2506>
- Burn, D. H. (1994). Hydrologic effects of climatic change in west-central Canada. *Journal of Hydrology*, 160(1–4), 53–70. [https://doi.org/10.1016/0022-1694\(94\)90033-7](https://doi.org/10.1016/0022-1694(94)90033-7)
- Burn, D. H. (1997). Catchment similarity for regional flood frequency analysis using seasonality measures. *Journal of Hydrology*, 202(1–4), 212–230. [https://doi.org/10.1016/S0022-1694\(97\)00068-1](https://doi.org/10.1016/S0022-1694(97)00068-1)
- Burn, D. H., & Elnur, M. (2002). Detection of hydrologic trends and variability. *Journal of Hydrology*, 255, 107–122. <https://doi.org/10.1533/9781845691127.2.485>
- Collins, M. J. (2019). River flood seasonality in the Northeast United States: Characterization and trends. *Hydrological Processes*, 33(5), 687–698. <https://doi.org/10.1002/hyp.13355>
- Court, A. (1952). Some new statistical techniques in geophysics. *Advances in Geophysics*, 1(C), 45–85. [https://doi.org/10.1016/S0065-2687\(08\)60204-6](https://doi.org/10.1016/S0065-2687(08)60204-6)
- Court, A. (1962). Measures of streamflow timing. *Journal of Geophysical Research*, 67(11), 4335–4339. <https://doi.org/10.1029/JZ067i11p04335>
- D'Agostino, R. B. (1970). Transformation to normality of the null distribution of g_1 . *Biometrika*, 57(3), 679–681.
- D'Agostino, R. B., Belanger, A., & D'Agostino, R. B. Jr. (1990). A suggestion for using powerful and informative tests of normality authors (s): Ralph B. D'Agostino, Albert Belanger, Ralph B. D'Agostino and Jr. Published by: Taylor & Francis, Ltd. on behalf of the American Statistical Association Stable U. *The American Statistician*, 44(4), 316–321. <https://doi.org/10.1080/00031305.1990.10475751>
- Dettinger, M. D., & Diaz, H. F. (2000). Global characteristics of stream flow seasonality and variability. *Journal of Hydrometeorology*, 1(4), 289–310. [https://doi.org/10.1175/1525-7541\(2000\)001%3C0289:GCOSFS%3E2.0.CO;2](https://doi.org/10.1175/1525-7541(2000)001%3C0289:GCOSFS%3E2.0.CO;2)
- Dhakal, N., Jain, S., Gray, A., Dandy, M., & Stancioff, E. (2015). Nonstationarity in seasonality of extreme precipitation: A nonparametric circular statistical approach and its application. *Water Resources Research*, 51, 4499–4515. <https://doi.org/10.1002/2014WR016399>
- Diehl, A. M. (2018). Timing is everything. *Nature Climate Change*, 8(10), 841–841. <https://doi.org/10.1038/s41558-018-0304-9>
- Do, H. X., Westra, S., & Leonard, M. (2017). A global-scale investigation of trends in annual maximum streamflow. *Journal of Hydrology*, 552, 28–43. <https://doi.org/10.1016/j.jhydrol.2017.06.015>
- Do, H. X., Gudmundsson, L., Leonard, M., & Westra, S. (2018). The global streamflow indices and metadata archive (GSIM)—Part 1: The production of a daily streamflow archive and metadata. *Earth System Science Data*, 10(2), 765–785. <https://doi.org/10.5194/essd-10-765-2018>
- Do, H. X., Westra, S., Leonard, M., & Gudmundsson, L. (2020). Global-scale prediction of flood timing using atmospheric reanalysis. *Water Resources Research*, 56(1), e2019WR024945. <https://doi.org/10.1029/2019WR024945>
- Dudley, R. W., Hodgkins, G. A., McHale, M. R., Kollian, M. J., & Renard, B. (2017). Trends in snowmelt-related streamflow timing in the conterminous United States. *Journal of Hydrology*, 547, 208–221. <https://doi.org/10.1016/j.jhydrol.2017.01.051>
- Durbin, J., & Watson, G. S. (1950). Testing for serial correlation in least squares regression. *Biometrika*, 37(3–4), 409–428.
- Fisher, N. I. (1993). *Statistical analysis of circular data*. New York, NY: Cambridge University Press. <https://doi.org/10.1017/CBO9780511564345>
- Formetta, G., Bell, V., & Stewart, E. (2018). Use of flood seasonality in pooling-group formation and quantile estimation: An application in Great Britain. *Water Resources Research*, 54, 1127–1145. <https://doi.org/10.1002/2017WR021623>
- Ganguli, P., Nandamuri, Y. R., & Chatterjee, C. (2019). Analysis of persistence in the flood timing and the role of catchment wetness on flood generation in a large river basin in India. *Theoretical and Applied Climatology*, 139(1–2), 373–388. <https://doi.org/10.1007/s00704-019-02964-z>
- GRDC. (2015). The global runoff data Centre. 56068 Koblenz, Germany.
- Gu, X., Zhang, Q., Singh, V. P., & Shi, P. (2017). Nonstationarity in timing of extreme precipitation across China and impact of tropical cyclones. *Global and Planetary Change*, 149, 153–165. <https://doi.org/10.1016/j.gloplacha.2016.12.019>
- Gudmundsson, L., Leonard, M., Do, H. X., Westra, S., & Seneviratne, S. I. (2019). Observed trends in global indicators of mean and extreme streamflow. *Geophysical Research Letters*, 46, 756–766. <https://doi.org/10.1029/2018GL079725>
- Gudmundsson, L., Do, H. X., Leonard, M., & Westra, S. (2018). The global streamflow indices and metadata archive (GSIM)—Part 2: Quality control, time-series indices and homogeneity assessment. *Earth System Science Data*, 10(2), 787–804. <https://doi.org/10.5194/essd-10-787-2018>
- Gumbel, E. J. (1941). The return period of flood flows. *The Annals of Mathematical Statistics*, 12(2), 163–190. <https://doi.org/10.1214/aoms/1177731747>
- Gumbel, E. J. (1954). Applications of the circular normal distribution. *Journal of the American Statistical Association*, 27(1), 267–297.
- Hall, J., Arheimer, B., Borga, M., Brázdil, R., Claps, P., Kiss, A., et al. (2014). Understanding flood regime changes in Europe: A state-of-the-art assessment. *Hydrology and Earth System Sciences*, 18(7), 2735–2772. <https://doi.org/10.5194/hess-18-2735-2014>
- Hall, J., & Blöschl, G. (2018). Spatial patterns and characteristics of flood seasonality in Europe. *Hydrology and Earth System Sciences*, 22(7), 3883–3901. <https://doi.org/10.5194/hess-22-3883-2018>
- Hamlet, A. F., & Lettenmaier, D. P. (2007). Effects of 20th century warming and climate variability on flood risk in the western U.S. *Water Resources Research*, 43, W06427. <https://doi.org/10.1029/2006WR005099>
- Head, L., Adams, M., McGregor, H., & Toole, S. (2014). Climate change and Australia. *Wiley Interdisciplinary Reviews: WIREs Climate Change*, 5(2), 175–197. Retrieved from <http://ro.uow.edu.au/cgi/viewcontent.cgi?article=1620&context=sspapers>
- Hidalgo, H. G., Das, T., Dettinger, M. D., Cayán, D. R., Pierce, D. W., Barnett, T. P., et al. (2009). Detection and attribution of streamflow timing changes to climate change in the Western United States. *Journal of Climate*, 22(13), 3838–3855. <https://doi.org/10.1175/2009JCLI2470.1>

- Hipel, K. W., & McLeod, A. I. (1994). *Time series modelling of water resources and environmental systems*. Amsterdam, The Netherlands: Elsevier.
- Hodgkins, G. A., & Dudley, R. W. (2006). Changes in the timing of winter-spring streamflows in eastern North America, 1913-2002. *Geophysical Research Letters*, 33, L06402. <https://doi.org/10.1029/2005GL025593>
- Klaus, S., Kreibich, H., Merz, B., Kuhlmann, B., & Schröter, K. (2016). Large-scale, seasonal flood risk analysis for agricultural crops in Germany. *Environmental Earth Sciences*, 75(18), 1289. <https://doi.org/10.1007/s12665-016-6096-1>
- Köplin, N., Schädler, B., Viviroli, D., & Weingartner, R. (2014). Seasonality and magnitude of floods in Switzerland under future climate change. *Hydrological Processes*, 28(4), 2567–2578. <https://doi.org/10.1002/hyp.9757>
- Koutroulis, A. G., Tsanis, I. K., & Daliakopoulos, I. N. (2010). Seasonality of floods and their hydrometeorologic characteristics in the island of Crete. *Journal of Hydrology*, 394(1–2), 90–100. <https://doi.org/10.1016/j.jhydrol.2010.04.025>
- Lee, D., Ward, P., & Block, P. (2015). Defining high-flow seasons using temporal streamflow patterns from a global model. *Hydrology and Earth System Sciences*, 19(11), 4689–4705. <https://doi.org/10.5194/hess-19-4689-2015>
- Linacre, E., & Geerts, B. (1997). *Climates & weather explained*. London; New York: Routledge.
- Marelle, L., Myhre, G., Hodnebrog, Ø., Sillmann, J., & Samsel, B. H. (2018). The changing seasonality of extreme daily precipitation. *Geophysical Research Letters*, 45, 11,352–11,360. <https://doi.org/10.1029/2018GL079567>
- Matti, B., Dahlke, H. E., Dieppois, B., Lawler, D. M., & Lyon, S. W. (2017). Flood seasonality across Scandinavia—Evidence of a shifting hydrograph? *Hydrological Processes*, 31(24), 4354–4370. <https://doi.org/10.1002/hyp.11365>
- Milly, P. C. D., Kam, J., & Dunne, K. A. (2018). On the sensitivity of annual streamflow to air temperature. *Water Resources Research*, 54, 2624–2641. <https://doi.org/10.1002/2017WR021970>
- Morán-Tejeda, E., Lorenzo-Lacruz, J., López-Moreno, J. I., Rahman, K., & Beniston, M. (2014). Streamflow timing of mountain rivers in Spain: Recent changes and future projections. *Journal of Hydrology*, 517, 1114–1127. <https://doi.org/10.1016/j.jhydrol.2014.06.053>
- Najafi, M. R., Zwiers, F. W., & Gillett, N. P. (2017). Attribution of observed streamflow changes in key British Columbia drainage basins. *Geophysical Research Letters*, 44, 11,012–11,020. <https://doi.org/10.1002/2017GL075016>
- Ouarda, T. B. M. J., Cunderlik, J. M., St-Hilaire, A., Barbet, M., Bruneau, P., & Bobée, B. (2006). Data-based comparison of seasonality-based regional flood frequency methods. *Journal of Hydrology*, 330(1–2), 329–339. <https://doi.org/10.1016/j.jhydrol.2006.03.023>
- Parajka, J., Kohnová, S., Bálint, G., Barbuc, M., Borga, M., Claps, P., et al. (2010). Seasonal characteristics of flood regimes across the Alpine-Carpathian range. *Journal of Hydrology*, 394(1–2), 78–89. <https://doi.org/10.1016/j.jhydrol.2010.05.015>
- Rao, V. B., Franchito, S. H., Santo, C. M. E., & Gan, M. A. (2016). An update on the rainfall characteristics of Brazil: Seasonal variations and trends in 1979-2011. *International Journal of Climatology*, 36(1), 291–302. <https://doi.org/10.1002/joc.4345>
- Schwarz, H. E. (1977). Climate change and water supply: How sensitive is the northeast? In *Climate, climatic change, and water supply* (pp. 111–120). Washington, DC: National Academy of Sciences.
- Sharma, A., Wasko, C., & Lettenmaier, D. P. (2018). If precipitation extremes are increasing, why aren't floods? *Water Resources Research*, 54, 8545–8551. <https://doi.org/10.1029/2018WR023749>
- Stahl, K., Tallaksen, L. M., Hannaford, J., & Van Lanen, H. A. J. (2012). Filling the white space on maps of European runoff trends: Estimates from a multi-model ensemble. *Hydrology and Earth System Sciences*, 16(7), 2035–2047. <https://doi.org/10.5194/hess-16-2035-2012>
- Stein, L., Pianosi, F., & Woods, R. (2020). Event-based classification for global study of river flood generating processes. *Hydrological Processes*, 34(7), 1514–1529. <https://doi.org/10.1002/hyp.13678>
- Stewart, I. T., Cayan, D. R., & Dettinger, M. D. (2005). Changes toward earlier streamflow timing across western North America. *Journal of Climate*, 18(8), 1136–1155. <https://doi.org/10.1175/JCLI3321.1>
- Tramblay, Y., Bouvier, C., Martin, C., Didon-Lescot, J. F., Todorovik, D., & Domergue, J. M. (2010). Assessment of initial soil moisture conditions for event-based rainfall-runoff modelling. *Journal of Hydrology*, 387(3–4), 176–187. <https://doi.org/10.1016/j.jhydrol.2010.04.006>
- Trenberth, K. E. (2011). Changes in precipitation with climate change. *Climate Research*, 47(1), 123–138. <https://doi.org/10.3354/cr00953>
- Ukkola, A. M., & Prentice, I. C. (2013). A worldwide analysis of trends in water-balance evapotranspiration. *Hydrology and Earth System Sciences*, 17(10), 4177–4187. <https://doi.org/10.5194/hess-17-4177-2013>
- Villarini, G. (2016). On the seasonality of flooding across the continental United States. *Advances in Water Resources*, 87, 80–91. <https://doi.org/10.1016/j.advwatres.2015.11.009>
- von Mises, R. (1918). Über die "Ganzzahligkeit" der Atomgewicht und verwandte Fragen. *Physikalische Zeitschrift*, 19, 490–500.
- Vormoor, K., Lawrence, D., Heistermann, M., & Bronstert, A. (2015). Climate change impacts on the seasonality and generation processes of floods—Projections and uncertainties for catchments with mixed snowmelt/rainfall regimes. *Hydrology and Earth System Sciences*, 19(2), 913–931. <https://doi.org/10.5194/hess-19-913-2015>
- Wasko, C., & Nathan, R. (2019). Influence of changes in rainfall and soil moisture on trends in flooding. *Journal of Hydrology*, 575, 432–441. <https://doi.org/10.1016/j.jhydrol.2019.05.054>
- Wasko, C., Nathan, R., & Peel, M. C. (2020). Changes in antecedent soil moisture modulate flood seasonality in a changing climate. *Water Resources Research*, 56, e2019WR026300. <https://doi.org/10.1029/2019WR026300>
- Wasko, C., & Sharma, A. (2017). Global assessment of flood and storm extremes with increased temperatures. *Scientific Reports*, 7, 7945. <https://doi.org/10.1038/s41598-017-08481-1>
- Wasko, C., Sharma, A., & Lettenmaier, D. P. (2019). Increases in temperature do not translate to increased flooding. *Nature Communications*, 10(1), 5676. <https://doi.org/10.1038/s41467-019-13612-5>
- Whitfield, P. H. (2012). Floods in future climates: A review. *Journal of Flood Risk Management*, 5(4), 336–365. <https://doi.org/10.1111/j.1753-318X.2012.01150.x>
- Wilks, D. S. (2006). On "field significance" and the false discovery rate. *Journal of Applied Meteorology and Climatology*, 45(9), 1181–1189. <https://doi.org/10.1175/JAM2404.1>
- Wilson, D., Hisdal, H., & Lawrence, D. (2010). Has streamflow changed in the Nordic countries?—Recent trends and comparisons to hydrological projections. *Journal of Hydrology*, 394(3–4), 334–346. <https://doi.org/10.1016/j.jhydrol.2010.09.010>
- Young, A. R., Round, C. E., & Gustard, A. (2000). Spatial and temporal variations in the occurrence of low flow events in the UK. *Hydrology and Earth System Sciences*, 4(1), 35–45. <https://doi.org/10.5194/hess-4-35-2000>
- Zhang, Q., Gu, X., Singh, V. P., Shi, P., & Luo, M. (2017). Timing of floods in southeastern China: Seasonal properties and potential causes. *Journal of Hydrology*, 552, 732–744. <https://doi.org/10.1016/j.jhydrol.2017.07.039>
- Zhang, X., Harvey, K. D., Hogg, W. D., & Yuzyk, T. R. (2001). Trends in Canadian streamflow. *Water Resources Research*, 37(4), 987–998. <https://doi.org/10.1029/2000WR900357>



Minerva Access is the Institutional Repository of The University of Melbourne

Author/s:

Wasko, C;Nathan, R;Peel, MC

Title:

Trends in Global Flood and Streamflow Timing Based on Local Water Year

Date:

2020-08-01

Citation:

Wasko, C., Nathan, R. & Peel, M. C. (2020). Trends in Global Flood and Streamflow Timing Based on Local Water Year. WATER RESOURCES RESEARCH, 56 (8), <https://doi.org/10.1029/2020WR027233>.

Persistent Link:

<http://hdl.handle.net/11343/264137>